International Journal of Engineering Science 167 (2021) 103514

Contents lists available at ScienceDirect

International Journal of Engineering Science

journal homepage: www.elsevier.com/locate/ijengsci

Coarse–grained modeling with hierarchical deformable and rigid assemblages (HiDRA)

A.Yu. Panchenko[a], E.A. Podolskaya[b,c], I.E. Berinskii[a,*]

[a] School of Mechanical Engineering, Tel Aviv Univeristy, Ramat Aviv, Tel Aviv 69978, Israel
[b] Institute for Problems in Mechanical Engineering RAS, 61, Bolshoy pr. V. O., St. Petersburg, 199178, Russia
[c] Peter the Great St. Petersburg Polytechnic University, 29, Politechnicheskaya str., St. Petersburg, 195251, Russia

ARTICLE INFO

Article history:
Received 25 January 2021
Revised 27 May 2021
Accepted 6 June 2021

Keywords:
Coarse-grained modeling
Multiscale modeling
Molecular dynamics

ABSTRACT

One of the major challenges in computational mechanics of materials remains to bridge the length-scale and time-scale gaps between the computational and experimental methods to study the microstructure of materials. Traditional molecular dynamics is a powerful tool at the nanoscale, but it does not allow to simulate such mechanical experiments as AFM microscopy dealing with sub-micrometric lengths and microsecond times. Coarse-grained (CG) modeling is one of the possible solutions to fill these gaps. CG modeling does not consider all atoms in a system, but the "pseudo-atoms" or "grains", approximating groups of these atoms. This allows a significant reduction in the number of considered interactions and degrees of freedom and, consequently, saves the computational resources.

In this work, the unique method for CG modeling named "Hierarchical Deformable and Rigid Assemblages" (HiDRA) is proposed. The grains are chosen as assemblages of the atoms in the original crystal lattice. The method allows incorporating the grains' elasticity so that the overall strain uniformly distributes in the lattice to avoid the unexpected stress concentrations in the bonds between the grains. Grains interact via forces acting to the surface atoms. Equations of motion for the grains are derived taking the uniform strain of the grain as an independent variable. In-house code is developed to perform the simulations with elastic grains. As an application, the HiDRA method is used to study the longitudinal vibrations and full 3D dynamics of chains of one-dimensional grains. Phonon spectra show to what extent large grains can correctly describe wave propagation in molecular chains.

1. Introduction

The rapid increase in the studies of new nanomaterials and nanostructures is not possible without the accurate and robust methods of microstructure properties investigation. A full description of these properties must include both experimental tests and computational simulations. Recent tremendous progress in the *in situ* measurements e.g., with transmission and scanning electron microscopes, makes it possible to characterize certain mechanical properties of the materials at nanoscale. At the same time, recent developments in spatial and temporal multiscale modeling have increased the size and duration of processes that can be simulated using accurate models for atomic interaction dramatically (Gerberich et al., 2017). How-

* Corresponding author.
E-mail address: igorbr@tauex.tau.ac.il (I.E. Berinskii).

https://doi.org/10.1016/j.ijengsci.2021.103514
0020-7225/

Fig. 1. The idea of CG modeling: the atomistic model (left), the atoms combined to super-atoms (middle), the CG model (right) (adopted from Chen et al. (2011)).

ever, computational nanomechanics still cannot describe the majority of the physical phenomena needed for engineering applications, so the gap in the length-scale and time-scale between the computational and experimental methods remains.

One of the most potent tools for theoretical investigation of materials at the nanoscale is **molecular dynamics (MD)** (Allen & Tildesley, 1989; Rapaport, 2004). In classical MD, atoms are represented as particles interacting with the forces determined from some interatomic potentials or force fields. The trajectories of the atoms are calculated using the numerical integration of Newton's equations of motion. Nowadays, MD simulations use parallel computing, allowing to handle more than 10^9 atoms (Chen, Zimmerman, Krivtsov, & McDowell, 2011), amounting to a volume less than a cubic micron, for a time scale of less than 1 μs. However, *the size of the systems considered in computational physics, chemistry and biology, and required simulation time scales are still too large to be studied in atomistic detail.* Therefore, **coarse–grained (CG) approaches** are used to represent the full system as a system with fewer degrees of freedom. In a general sense, classical thermodynamics and continuum mechanics can also be considered as coarse-grained theories, as well as multiple scale modeling methods such as quasi-continuum method (Kochmann & Amelang, 2016; Miller & Tadmor, 2002), MAAD (Abraham, Broughton, Bernstein, & Kaxiras, 1998), CADD (Shilkrot, Miller, & Curtin, 2004), bridging domain (Xiao & Belytschko, 2004), bridging scale (Liu et al., 2006), atomistic field theory (Chen & Lee, 2005), and many others. The methods mentioned above use the mixed continuum and atomistic approach to represent the material's structure. In contrast, we consider CG models in a narrower sense, as a reduced representation of the atomistic structure. The number of atoms is lowered by combining them into the "super–atoms" or "grains" (Fig. 1). The inner structure of the grain is therefore neglected, and all the corresponding degrees of freedom are excluded. At the same time, material still does not use any continuum representation, and all simulations are performed in the frames of the same discrete approach. Simplified CG-representation is widely used to simulate biomolecular systems (Noid, 2013) including biomembranes (Shi, Kong, & Gao, 2008), and proteins (Gautieri, Russo, Vesentini, Redaelli, & Buehler, 2010; Kmiecik et al., 2016); liquid crystals (Care & Cleaver, 2005; Wilson, 2005), carbon nanotubes (Ostanin, Dumitrică, Eibl, & Rüde, 2019), etc. The relevance of CG calculations was confirmed by the recent Nobel Prize in chemistry given to Michael Levitt, Martin Karplu, and Arieh Warshel for their pioneering multiscale models for complex chemical systems (Levitt & Chothia, 1976; Warshel & Levitt, 1976). Being coupled with the finite element method, coarse–grained molecular dynamics (CGMD) can be a powerful tool in the mechanics of materials (Rudd & Broughton, 1998).

The interaction between the grains is determined by the empirical potential. This potential plays the same role in the mechanics of discrete systems as the constitutive relations in continuum mechanics; namely, it approximates the system's response to external stimuli. Usually, it depends on the positions of the interacting grains. In such cases grains are considered as materials points, and the interaction is fully described by forces acting from one grain to the others. But often, *the orientations of the grains must be taken into account*. In these cases, the **rotational degrees of freedom** must be considered in addition to the translational ones (see Ivanova, 2018) and references therein). In general, this corresponds to the consideration of the grain as a rigid body. The interaction between such rigid grains is then determined not only by the forces but also by the torques.

We propose a new CG modeling method referred to as "Hierarchical Deformable and Rigid Assemblages" (**HiDRA**). The method bases on two principles. Firstly, the grains are chosen as assemblages of the atoms in the original crystal lattice. Using the periodicity of the crystal lattice, it is possible to increase the size of the grains hierarchically. In this case, the smaller grains are nested in the bigger ones. The modeled system can then include the small grains and even single atoms in the regions of interest (defects, crack tips, stress risers) combined with the large grains in other regions providing the multiscale consideration. Secondly, the grains can be considered either as rigid or solid bodies. These features are discussed below.

The original way to simulate a crystal lattice with grains was proposed recently by Panchenko, Podolskaya, and Berinskii (2020). The grains were combined from the rigidly connected atoms of the original atomic lattice. In this case, the simulation time reduction in comparison with the fully atomistic MD should be proportional to $(R/a)^3$, where R is a grain's characteristic length and a is an interatomic distance. The method was used to simulate nanoindentation of single-layer molybdenum disulfide ($SLMoS_2$). The interaction of the grains was derived from the forces acting between the surface atoms. In particular, it was shown that although the rigid grains can be successfully used for a large class of problems, in some cases, they lead to the wrong description of material properties. Fixing the distances between the atoms makes the lattice much stiffer. As a result, it is necessary to re-calibrate the interatomic potentials to comply with the homogenized elastic properties of the original crystal lattice. However, this leads to the incorrect prediction of the phonon spectra of the original lattice. Also, if the lattice is stretched, a rigid grain cannot elongate, so all the effective strain is transferred to the bonds between the grains. As a result, the bonds reach the critical strain too fast, leading to the material's premature fracture as

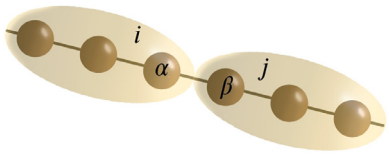

Fig. 2. Schematic representation of a pair of interacting grains i and j.

it was demonstrated in Panchenko et al. (2020). Finally, it is not natural to represent a grain with a rigid structure in soft matter modeling.

A possible solution is to consider not rigid but **solid grains**, prone to uniform elastic strain. This idea has several advantages. Firstly, in this case, it is not necessary to re-calibrate the interatomic potential for specific grains. Instead, only the stiffness of the isotropic grain must be found. Moreover, in this case, the interatomic potential can describe the interaction of the grains of different sizes (combining more or fewer atoms) and interaction between the grains and single atoms. It can be used for the mixed representation of the crystal lattice so that it is modeled with atoms in the areas of stress concentration and with the coarse grains in less critical areas. Secondly, in the case of deformable solid grain, the overall strain uniformly distributes in the lattice, which helps to avoid the unexpected stress concentrations in the bonds between the grains.

Deformation of the particles has been introduced in many ways in the discrete element method (see Rojek, Zubelewicz, Madan, & Nosewicz, 2018 and references therein) and the movable cellular automaton method (Psakhie et al., 2014; Psakhie et al., 2011). In all these papers, deformation of the particles is caused by the contact forces containing central and tangential constituents. Hence, the strain is caused by the overlapping of the particles, and, in general, consists of the central, tangential, and volume-dependent contributions. In our case, the solid particles *do not overlap*, and their deformation is caused by multibody interaction between the surface atoms. Also, the approaches mentioned above are based on the quasi-static solutions for the strains of the elements that fulfill the equilibrium conditions at every time step. In contrast, the strain tensor components are considered *independent variables* in the present work, and they are determined as a solution to the coupled dynamical equations of motion.

The use of deformable grain is a compromise solution combining the speed of the coarse models and the accuracy of full-scale models. In continuum mechanics, the use of deformable particles leads to the micromorpic theory, proposed by Eringen and Suhubi (1964), and it is successfully used in nanomechanical problems (Chen, Lee, & Eskandarian, 2004; Wang & Lee, 2010). However, for discrete coarse-grained modeling, the approach based on the use of elastic particles has not been developed yet. In this work, we derive the general equations of motion of the deformable solid grains. As a first implementation, we apply this method to study the dynamics of one-dimensional grains.

2. General equations for the CG modeling with deformable solid grains

Suppose that the strain tensor $\boldsymbol{\varepsilon}_i$ is uniform inside the grain. The current position of an atom α belonging to the grain i (see Fig. 2) is calculated as:

$$\begin{aligned} \mathbf{r}_\alpha &= \mathbf{r}_i + \mathbf{P}_i \cdot \mathbf{r}_{i\alpha}, \\ \mathbf{r}_{i\alpha} &= (\mathbf{E} + \boldsymbol{\varepsilon}_i) \cdot \mathbf{r}^0_{i\alpha} \end{aligned} \tag{1}$$

where $\mathbf{r}_i$ is the position vector of the center of mass of the grain i, $\mathbf{r}_{i\alpha}$ gives the position of atom α relative to the center of mass of the grain i, and tensor $\mathbf{P}_i$ determines the rotation of the grain. The superscript 0 denotes the reference configuration. The respective velocity is equal to

$$\dot{\mathbf{r}}_\alpha = \dot{\mathbf{r}}_i + \mathbf{P}_i \cdot (\boldsymbol{\omega}_i \times \mathbf{r}_{i\alpha}) + \mathbf{P}_i \mathbf{r}^0_{i\alpha} \cdot\cdot \dot{\boldsymbol{\varepsilon}}_i \tag{2}$$

where $\boldsymbol{\omega}_i$ is the angular velocity, and the kinetic energy of atomic motion for the grain i yields to:

$$T_i = \sum_\alpha \frac{m_\alpha}{2} \dot{\mathbf{r}}_\alpha \cdot \dot{\mathbf{r}}_\alpha \tag{3}$$

Next, the potential energy is also required:

$$U_i = \sum_{j \neq i, \alpha, \beta} \Pi_{\alpha\beta} + \frac{V}{2} \boldsymbol{\varepsilon}_i \cdot\cdot {}^4\mathbf{C} \cdot\cdot \boldsymbol{\varepsilon}_i, \tag{4}$$

where ${}^4\mathbf{C}$ is the stiffness tensor of the grain. The first term is determined by the forces between the grains, whereas the second one originates from the grains deformation. The notation $\Pi_{\alpha\beta}$ is used for the pair interaction potential between atom α from grain i and atom β from grain j, however, the subsequent considerations are not restricted by the type of the potential.

We use Lagrange formalism to construct the equations of motion, and vector and tensor analogues of **Euler-Lagrange equations** are written down. The derivatives of the kinetic and potential energies with respect to three generalized coordinates and their rates, i.e. **center of mass position** for grain i, its **rotation** and **deformation**, are given in the Appendix.

It should be noted that the force of pair interaction $\mathbf{F}_{ij}$ acting to the grain i from the grain j can be found as a sum of forces acting to the atoms α, belonging to grain i, from the atoms β which belong to grain j (see Fig. 2):

$$\mathbf{F}_{ij} = \sum_{\alpha,\beta} \mathbf{F}_{\alpha\beta} = \sum_{\alpha,\beta} \frac{\partial \Pi_{\alpha\beta}}{\partial \mathbf{r}_{\alpha\beta}}. \tag{5}$$

Note that this formula is written in the fixed frame. In what follows, we derive the formulae for torques $\mathbf{M}_{ij}$ and stresses, both internal $\boldsymbol{\sigma}_i^{int}$ and external $\boldsymbol{\sigma}_i^{ext}$, in the coordinate system associated with grain. Then, the force $\mathbf{F}_{\alpha\beta}$ has to be written in this coordinate system:

$$\mathbf{F}_{i,\alpha\beta} = \mathbf{P}_i^T \cdot \mathbf{F}_{\alpha\beta}, \tag{6}$$

and the pair torque acting to the grain i from the grain j and calculated relative to the center of mass of i is

$$\mathbf{M}_{ij} = \sum_{\alpha,\beta} \mathbf{r}_{i\alpha} \times \mathbf{F}_{i,\alpha\beta}. \tag{7}$$

Finally, we obtain three differential equations that fully describe the motion of the lattice with "deformable" grains:

$$\ddot{\mathbf{r}}_i \sum_{\alpha} m_\alpha = \sum_{j\neq i} \mathbf{F}_{ij} \tag{8}$$

$$\mathbf{J}_i \cdot \dot{\boldsymbol{\omega}}_i + \left(2\dot{\boldsymbol{\varepsilon}}_i \cdot \widehat{\mathbf{J}}_i \mathbf{E} - \dot{\boldsymbol{\varepsilon}}_i \cdot \widehat{\mathbf{J}}_i - \widehat{\mathbf{J}}_i \cdot \dot{\boldsymbol{\varepsilon}}_i\right) \cdot \boldsymbol{\omega}_i + \dot{\boldsymbol{\varepsilon}}_i \cdot \cdot \left(\dot{\boldsymbol{\varepsilon}}_i \cdot \widetilde{\mathbf{J}}_i \times \mathbf{E}\right) - \ddot{\boldsymbol{\varepsilon}}_i \cdot \cdot \left(\widehat{\mathbf{J}}_i^T \times \mathbf{E}\right) = \sum_{j\neq i} \mathbf{M}_{ij} \tag{9}$$

$$\begin{aligned} &\frac{1}{2}\left(\ddot{\boldsymbol{\varepsilon}}_i \cdot \widetilde{\mathbf{J}}_i + \widetilde{\mathbf{J}}_i \cdot \ddot{\boldsymbol{\varepsilon}}_i\right) + \frac{1}{2}\left(\dot{\boldsymbol{\omega}}_i \times \widehat{\mathbf{J}}_i^T - \widehat{\mathbf{J}}_i \times \dot{\boldsymbol{\omega}}_i\right) + \frac{1}{2}\left(\boldsymbol{\omega}_i \times \dot{\boldsymbol{\varepsilon}}_i \cdot \widetilde{\mathbf{J}}_i - \widetilde{\mathbf{J}}_i \cdot \dot{\boldsymbol{\varepsilon}}_i \times \boldsymbol{\omega}_i\right) - \frac{1}{2}\left[\omega_i^2\left(\widehat{\mathbf{J}}_i + \widehat{\mathbf{J}}_i^T\right) - \boldsymbol{\omega}_i \cdot \widehat{\mathbf{J}}_i^T \boldsymbol{\omega}_i - \boldsymbol{\omega}_i \widehat{\mathbf{J}}_i \cdot \boldsymbol{\omega}_i\right] \\ &-\frac{1}{2}\sum_{\alpha} m_\alpha \dot{\boldsymbol{\varepsilon}}_i \cdot \cdot (\boldsymbol{\omega}_i \times \mathbf{e}_r)\mathbf{r}_{i\alpha}^0\left[\mathbf{r}_{i\alpha}^0 \mathbf{e}_r + \mathbf{e}_r \mathbf{r}_{i\alpha}^0\right] = V\left(\boldsymbol{\sigma}_i^{int} - \boldsymbol{\sigma}_i^{ext}\right) \end{aligned} \tag{10}$$

Here we introduce three auxiliary tensors $\mathbf{J}_i$, $\widetilde{\mathbf{J}}_i$ and $\widehat{\mathbf{J}}_i$

$$\begin{aligned} \mathbf{J}_i &= \sum_{\alpha} m_\alpha\left[(r_{i\alpha})^2 \mathbf{E} - \mathbf{r}_{i\alpha}\mathbf{r}_{i\alpha}\right] \\ \widetilde{\mathbf{J}}_i &= \sum_{\alpha} m_\alpha \mathbf{r}_{i\alpha}^0 \mathbf{r}_{i\alpha}^0 \\ \widehat{\mathbf{J}}_i &= \sum_{\alpha} m_\alpha \mathbf{r}_{i\alpha}^0 \mathbf{r}_{i\alpha} \end{aligned} \tag{11}$$

Tensor $\mathbf{J}_i$ is the inertia tensor of the grain i in the current configuration, and for the sake of simplicity we will further refer to the others as inertia tensors as well.

3. CG modelling for 3D motion of a chain of atoms

Let us apply the suggested method to the investigation of the 3D motion of a chain of atoms connected with the elastic springs.

As an example suppose that we combine two atoms in a grain, so that α is equal either to 1 or to 2. Moreover, let $m_1 = m_2 = m$, so the position vector of the grain's center of mass $\mathbf{r}_i$ and the position vectors of atoms (1) obey the following equalities in the current configuration

$$\mathbf{r}_i = \frac{1}{2}(\mathbf{r}_1 + \mathbf{r}_2), \qquad \mathbf{r}_{i1} = -\mathbf{r}_{i2}, \qquad \mathbf{r}_1 - \mathbf{r}_2 = 2\mathbf{P}_i \cdot \mathbf{r}_{i1} \tag{12}$$

Let the initial chain be aligned along the axis $\mathbf{e}_x$. Then

$$\mathbf{r}_1^0 - \mathbf{r}_2^0 = a\mathbf{e}_x, \qquad \mathbf{r}_{i1}^0 = \frac{1}{2}a\mathbf{e}_x, \qquad \mathbf{r}_{i1} = \frac{1}{2}(1+\varepsilon_i)a\mathbf{e}_x \tag{13}$$

Here ε_i is the strain, a is the equilibrium distance between the nearest atoms, and superscript 0 corresponds to the reference configuration.

The chain is one-dimensional, and as in (1) deformation is carried out prior to rotation, the strain tensor yields to

$$\boldsymbol{\varepsilon}_i = \varepsilon_i \mathbf{e}_x \mathbf{e}_x \tag{14}$$

Then, the Eqs. (1) and (2) are simplified. Respectively, the current positions of atoms are given by

$$\begin{aligned}\mathbf{r}_1 &= \mathbf{r}_i + \frac{1}{2}(1+\varepsilon_i)a\mathbf{P}_i\cdot\mathbf{e}_x,\\ \mathbf{r}_2 &= \mathbf{r}_i - \frac{1}{2}(1+\varepsilon_i)a\mathbf{P}_i\cdot\mathbf{e}_x\end{aligned} \tag{15}$$

and their velocities are equal to

$$\begin{aligned}\dot{\mathbf{r}}_1 &= \dot{\mathbf{r}}_i + \frac{1}{2}a\Big[(1+\varepsilon_i)\boldsymbol{\omega}_i\times\mathbf{E} + \dot{\varepsilon}_i\mathbf{E}\Big]\cdot\mathbf{P}_i\cdot\mathbf{e}_x,\\ \dot{\mathbf{r}}_2 &= \dot{\mathbf{r}}_i - \frac{1}{2}a\Big[(1+\varepsilon_i)\boldsymbol{\omega}_i\times\mathbf{E} + \dot{\varepsilon}_i\mathbf{E}\Big]\cdot\mathbf{P}_i\cdot\mathbf{e}_x\end{aligned} \tag{16}$$

The inertia tensors (11) take the form

$$\mathbf{J}_i = \frac{1}{2}ma^2(1+\varepsilon_i)^2(\mathbf{E}-\mathbf{e}_x\mathbf{e}_x) \qquad \widetilde{\mathbf{J}}_i = \frac{1}{2}ma^2\mathbf{e}_x\mathbf{e}_x \qquad \widehat{\mathbf{J}}_i = \frac{1}{2}ma^2(1+\varepsilon_i)\mathbf{e}_x\mathbf{e}_x \tag{17}$$

Eventually, the equation of motion for the grain's center of mass (8) remains the same

$$2m\ddot{\mathbf{r}}_i = \sum_{j\neq i}\mathbf{F}_{ij} \tag{18}$$

The respective external forces are determined by the particular interaction law (5).

Assuming that the chain does not revolve around its axis, i.e.

$$\omega_{ix} = 0,$$

taking into account that

$$\mathbf{e}_x\mathbf{e}_x\cdot\cdot(\mathbf{e}_x\mathbf{e}_x\times\mathbf{E}) \equiv 0$$

$$\boldsymbol{\omega}_i\times\mathbf{E} = \omega_{iy}(\mathbf{e}_x\mathbf{e}_z - \mathbf{e}_z\mathbf{e}_x) + \omega_{iz}(\mathbf{e}_y\mathbf{e}_x - \mathbf{e}_x\mathbf{e}_y),$$

and substituting (12)–(17) into (9), we obtain

$$\frac{1}{2}(1+\varepsilon_i)^2\big(\dot{\omega}_{iy}\mathbf{e}_y + \dot{\omega}_{iz}\mathbf{e}_z\big) + (1+\varepsilon_i)\dot{\varepsilon}_i\big(\omega_{iy}\mathbf{e}_y + \omega_{iz}\mathbf{e}_z\big) = \frac{1}{ma^2}\sum_{j\neq i}\mathbf{M}_{ij}, \tag{19}$$

where the torques are calculated according to (7).

Finally, the third equation of motion (10) yields to

$$\begin{aligned}&\frac{1}{2}\big(\ddot{\varepsilon}_i + \omega_{iy}^2 + \omega_{iz}^2\big)\mathbf{e}_x\mathbf{e}_x + \frac{1}{2}\dot{\varepsilon}_i\big[\omega_{iz}(\mathbf{e}_y\mathbf{e}_x + \mathbf{e}_x\mathbf{e}_y) - \omega_{iy}(\mathbf{e}_x\mathbf{e}_z + \mathbf{e}_z\mathbf{e}_x)\big]\\ &\quad + (1+\varepsilon_i)\big[\dot{\omega}_{iz}(\mathbf{e}_y\mathbf{e}_x + \mathbf{e}_x\mathbf{e}_y) - \dot{\omega}_{iy}(\mathbf{e}_x\mathbf{e}_z + \mathbf{e}_z\mathbf{e}_x)\big] = \frac{1}{ma^2}V\big(\boldsymbol{\sigma}_i^{int} - \boldsymbol{\sigma}_i^{ext}\big)\end{aligned} \tag{20}$$

To conclude the derivation, consider the external stress acting to the grain. It can be calculated using formula (58):

$$\boldsymbol{\sigma}_i^{ext} = \frac{a}{8V}\sum_{j\neq i,\beta}\Big[\mathbf{e}_x\big(\mathbf{F}_{i,1\beta} - \mathbf{F}_{i,2\beta}\big) + \big(\mathbf{F}_{i,1\beta} - \mathbf{F}_{i,2\beta}\big)\mathbf{e}_x\Big] \tag{21}$$

where $\mathbf{F}_{i,1\beta}$ and $\mathbf{F}_{i,2\beta}$ are the forces acting to the given grain from the atom β (from grain j) and written in the frame associated with the grain i (6), and $V = a$ is the volume of the grain, i.e. its length, in the reference configuration.

For the internal stresses we take the formula for stiffness tensor, again, determined by the particular interaction law. E.g. if the bond inside the grain possesses both longitudinal and transverse stiffnesses c_L and c_T, the stiffness tensor will take the form Ivanova, Krivtsov, and Morozov (2007)

$${}^4\mathbf{C} = a((c_L - c_T)\mathbf{e}_x\mathbf{e}_x\mathbf{e}_x\mathbf{e}_x + c_T\mathbf{e}_x\mathbf{E}\mathbf{e}_x), \tag{22}$$

and

$$\boldsymbol{\sigma}_i^{int} = {}^4\mathbf{C}\cdot\cdot\boldsymbol{\varepsilon}_i = a\varepsilon_i c_L\mathbf{e}_x\mathbf{e}_x. \tag{23}$$

Note that for the chain only longitudinal stiffness of the grain is accounted for in the respective equations of motion. Thus, the shear stresses which originate from strain rate and angular acceleration of the grain match only those of the $\boldsymbol{\sigma}_i^{ext}$.

4. Longitudinal vibrations of CG chain. Arbitrary size of the grain

Let the "initial" grain now contain N atoms of the original chain, so its length is $l_0 = (N-1)a$. For the sake of simplicity, we further restrict ourselves to the analysis of longitudinal vibrations, i.e. pure one-dimensional motion, and only the nearest neighbor interaction.

Effective models Let us try to derive the equations of motion for the 1D CG chain from a different angle. We replace the polyatomic grain with a diatomic one with just two pseudoatoms located at the edges of the grain. There are two ways to do that: we can (i) either keep all the inertia characteristics of the grain or (ii) only its moment of inertia and its size. As a result we obtain two different effective models of the CG chain.

In both cases the masses of the atoms are redistributed. So in case (i), the masses of the pseudoatoms M and the length of the new grain l need to be determined to equalize the total mass and the moment of inertia of the initial grain and the new one:

$$M = \frac{1}{2}\sum_{\alpha} m_\alpha \qquad l = \sqrt{\frac{2}{M}\sum_{\alpha} m_\alpha r_{i\alpha}^2}. \tag{24}$$

In the case (ii) we keep the length of the grain and find the masses M that equalize only the moment of inertia:

$$l \equiv l_0, \qquad M = \frac{2\sum\limits_{\alpha} m_\alpha r_{i\alpha}^2}{l_0^2}. \tag{25}$$

In pure one-dimensional case the grains are not subject to any rotations, so the equations of motion are determined by the displacements of the pseudoatoms u_i and v_i:

$$M\ddot{u}_i = F(v_i - u_i) - F(u_i - v_{i-1}) \qquad M\ddot{v}_i = F(u_{i+1} - v_i) - F(v_i - u_i) \tag{26}$$

Here $F(v_i - u_i)$ is the elastic force in a bond connecting the pseudoatom with a displacement v_i and the pseudoatom with a displacement u_i. Let us represent their current positions as:

$$r_1 = r_i^0 - \frac{1}{2}l + u_i = r_i - \frac{1}{2}l(1+\varepsilon_i) \qquad r_2 = r_i^0 + \frac{1}{2}l + v_i = r_i + \frac{1}{2}l(1+\varepsilon_i) \tag{27}$$

Here ε_i is the strain of the grain, r_i^0 and r_i are the positions of the grain's center of mass at the reference and actual configurations, and we use the same index notation as in the previous paragraphs. Equation (27) correspond to the Eq. (1) in 1D case. Substitution to the system (26) gives:

$$2\ M\ \ddot{r}_i = F(u_{i+1} - v_i) - F(u_i - v_{i-1}) = F_i^{ext} \tag{28}$$

Here F_i^{ext} is actually the sum of the external forces acting on the grain i.

The equation featuring torques degenerates in one-dimensional case, so we pass over to the last equation obtained by substraction of the first equation of the system (26) from the second one:

$$M\ l\ \ddot{\varepsilon}_i = (F(u_{i+1} - v_i) + F(u_i - v_{i-1})) - 2\ F(v_i - u_i) \tag{29}$$

Next, consider the stress tensors (21) and (23). The volume of the grain is equal to its length, i.e. $V = l$, and the distance between the nearest neighbors is $l/2$. Hence, the only one component of the external stress tensor is equal to

$$\sigma^{ext} = \frac{1}{2}\ (F(u_{i+1} - v_i) + F(u_i - v_{i-1})) \tag{30}$$

At the same time, it can be noticed that the internal stress can be found either using formula (23), or as a derivative of the strain energy by $\varepsilon_i = (v_i - u_i)/l$:

$$\sigma^{int} = F(v_i - u_i) \tag{31}$$

Using this and multiplying (29) by a, we obtain

$$\frac{1}{2}M\ l^2\ddot{\varepsilon}_i = V(\sigma^{ext} - \sigma^{int}). \tag{32}$$

Influence of grain size on the phonon spectra As noted in Chen et al. (2011) a simple equivalent structural representation averages out the fine details of the molecular structure and high-frequency vibrations of the systems. There is an open question, however, to what extent CG models can be used the phonon spectra of the fully atomic systems. Let us consider the one-dimensional example from the previous section to analyze how the size of the grain affects the wave propagation in the material. The one-dimensional crystal is represented as 1D chain of diatomic grains. Equations (28) and (29) can be rewritten in terms of a center of mass displacement and a strain, taking into account

$$\begin{aligned} &F_1(u_{i+1} - v_i) = c_1(r_{i+1} - r_i - a - \frac{1}{2}l(2 + \varepsilon_{i+1} + \varepsilon_i)) \\ &F_1(u_i - v_{i-1}) = c_1(r_i - r_{i-1} - a - \frac{1}{2}l(2 + \varepsilon_i + \varepsilon_{i-1}))F_2(v_i - u_i) = c_2(l\varepsilon_i), \qquad c_2 = \frac{1}{2}c_1. \end{aligned} \tag{33}$$

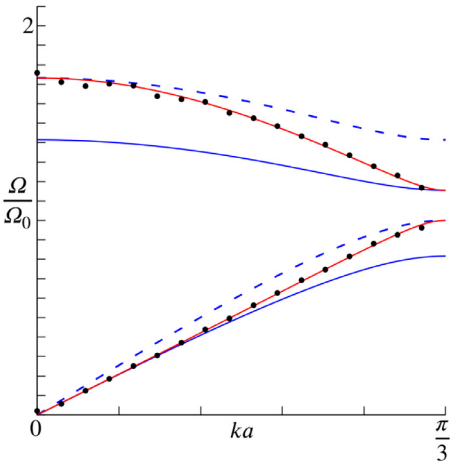

Fig. 3. Phonon spectrum for the monoatomic chain: effective inertia model (blue solid line), effective size model (blue dashed line), HiDRA model (red solid line), simulation (black dots). (For interpretation of the references to colour in this figure legend, the reader is referred to the web version of this article.)

Here c_2 is chosen so that the effective stiffness of the grain remains the same as a stiffness of the interatomic bond in the original chain. Now, solutions of the rewritten Eqs. (28) and (29) can be found as the traveling waves

$$r_n = r_0 \exp\left(\mathbf{i}(-\Omega t + knL)\right) \qquad \varepsilon_n = \varepsilon_0 \exp\left(\mathbf{i}(-\Omega t + knL)\right) \tag{34}$$

where $L = l_0 + a$ is a period of the chain. This allows obtaining the dispersion curves, which are discussed below.

It can be easily shown that if a diatomic grain contains 2 atoms of the original lattice, then the models coincide and one obtains the exact solution as expected, because the combination of the acoustic and the optical spectra for the diatomic elastic grains gives the full acoustic spectrum of the original chain.

Consider now a diatomic grain which contains three atoms of the original lattice. Figure 3 shows the phonon spectra obtained within four approaches. The vertical axis is normalized to the oscillation frequency of a pair of atoms in a monoatomic chain $\Omega_0 = \sqrt{\frac{c_1}{m}}$, and $a = \dfrac{L}{3}$ is the respective interatomic distance in the reference configuration.

The effective inertia model (blue solid line) and the effective size model (blue dashed line) refer, respectively, to case (i) matching all the inertia characteristics of the grain and case (ii) keeping its size. Black dots show the results of CG simulation, for which the details are given in the next section. Note that the simulation results lie exactly in between the effective models and coincide with the analytical results given by the HiDRA model (red solid line). Let us not, that this model can be considered as a "mixed" model which incorporates the equation of motion for the grain's center of mass from the effective inertia model, whereas the equation for the strain is taken from the effective size model.

5. Simulation technique

The main idea of the simulations method is close to the distinct (Ostanin et al., 2019) and discrete (Cundall & Strack, 1979) element methods and other generalizations of classical molecular dynamics. The grains are simulated as solids with given masses and moments of inertia. In what follows, we take the characteristics of these solids and the forces, torques and stresses as in Sections 2 and 3.

Dynamics of the grains The position of the center of mass of specific grain i is determined by the solution of the equation of motion (8). Then, generally speaking, the angular acceleration and "strain acceleration" of this grain can be found by solving system of Eqs. (9) and (10). Next, we determine the angular velocity and strain rate by integration of the corresponding accelerations at each time step $\mathrm{dt} = 0.005\mathrm{T}_0$ using leap–frog algorithm (Allen & Tildesley, 1989). Here $T_0 = \frac{2\pi}{\Omega_0}$ is the period of oscillations of a pair of atoms in a monoatomic chain, and $\Omega_0 = \sqrt{\frac{c_0}{m_0}}$, c_0 and m_0 are the reference parameters.

As far as the rotational degrees of freedom are concerned, we apply the quaternions formalism (Altmann, 1986). We introduce a unit vector $\mathbf{w}_i$ which determines the axis of rotation at current time step. Hence, the rotation around the vector $\mathbf{w}_i$ is calculated at each time step $\mathbf{d}t$ using quaternions $\mathbf{q}_i$ as:

$$\mathbf{q}_i(t + \mathrm{dt}) = \mathbf{q}_i(t) * \mathrm{d}\mathbf{q}_\mathrm{i}, \tag{35}$$

where

$$\mathrm{d}\mathbf{q}_\mathrm{i} = \cos\left(\frac{\omega_\mathrm{i}\mathrm{dt}}{2}\right) + \mathbf{w}_\mathrm{i}\sin\left(\frac{\omega_\mathrm{i}\mathrm{dt}}{2}\right). \tag{36}$$

For small rotations, the latter yields to:

$$\mathrm{d}\mathbf{q_i} = 1 - \frac{1}{2}\left(\frac{\boldsymbol{\omega_i}\mathrm{dt}}{2}\right)^2 + \boldsymbol{\omega_i}\frac{\mathrm{dt}}{2}. \tag{37}$$

Additionally, quaternions $\mathbf{q}_i$ are normalized at every step.

Hence, the rotation of vectors $\mathbf{r}_{i\alpha}$ is calculated as

$$\mathbf{P}_i \cdot \mathbf{r}_{i\alpha} = \mathbf{q}_i * \mathbf{r}_{i\alpha} * \mathbf{q}_i^{-1}. \tag{38}$$

and the rotation tensor $\mathbf{P}_i$ has the following components

$$\mathbf{P}_i \sim \begin{pmatrix} q_{i,0}^2 + q_{i,x}^2 - q_{i,y}^2 - q_{i,z}^2 & 2q_{i,x}q_{i,y} - 2q_{i,0}q_{i,z} & 2q_{i,x}q_{i,z} + 2q_{i,0}q_{i,y} \\ 2q_{i,x}q_{i,y} + 2q_{i,0}q_{i,z} & q_{i,0}^2 - q_{i,x}^2 + q_{i,y}^2 - q_{i,z}^2 & 2q_{i,y}q_{i,z} - 2q_{i,0}q_{i,x} \\ 2q_{i,x}q_{i,z} - 2q_{i,0}q_{i,y} & 2q_{i,y}q_{i,z} + 2q_{i,0}q_{i,x} & q_{i,0}^2 - q_{i,x}^2 - q_{i,y}^2 + q_{i,z}^2 \end{pmatrix}. \tag{39}$$

Elasticity of the CG chain. Phonon spectrum Without loss of generality we can assume that initial distance between the atoms in grain is the same. So for the linear interaction between the atoms, the stiffness of the grain, which is further required for the calculation of the internal stresses (23), does not depend on the number of atoms in the grain.

Passing over to the chain of atoms connected with the elastic springs, we obtain the grain's longitudinal stiffness

$$c_L = n\left(\sum_i^n \frac{1}{c_i}\right)^{-1}, \tag{40}$$

where n is the number of interactions in grain, c_i is the respective bond's stiffness. For a monoatomic chain $c_i \equiv c_0$.

In order to validate the system dynamics, we use the phonon spectrum. The phonon spectrum of the CG chain is measured using an approach based on molecular dynamics simulations (Kong, 2011). Namely, we apply the Langevin thermostat for grains by generalization of damping term, whereas the random term is calculated as a sum of random forces acting on the atoms belonging to the grains. The coarse–grained lattice has 2 degrees of freedom in 1D case (1 translational DOF and 1 strain) and 6 degrees of freedom in 3D case (3 translational DOF, 2 rotational DOF, because we exclude the rotation around the grain's axis, and 1 strain). Hence, following (Altmann, 1986) we introduce the respective generalized displacements $\widetilde{\mathbf{u}}_i$ and generalized velocities $\widetilde{\boldsymbol{\upsilon}}_i$ for each grain i.

The generalized displacements in the reciprocal space are defined as the Fourier transform of displacements in the real space

$$\widetilde{\mathbf{u}}(\mathbf{k}) = \frac{1}{\sqrt{N}}\sum_i \widetilde{\mathbf{u}}_i \exp\left(-\mathbf{i}\mathbf{k}\cdot\mathbf{r}_i\right) \tag{41}$$

where N is the number of grains, $\mathbf{k}$ is a wave vector. The Green's tensor is calculated as the time average of the tensor product $\widetilde{\mathbf{u}}(\mathbf{k})$ with its complex conjugate $\widetilde{\mathbf{u}}^*(\mathbf{k})$:

$$\mathbf{G}(\mathbf{k}) = \langle \widetilde{\mathbf{u}}(\mathbf{k})\widetilde{\mathbf{u}}^*(\mathbf{k})\rangle \tag{42}$$

Finally, the dynamical tensor $\mathbf{D}(\mathbf{k})$ is proportional to the inverse of the Green's tensor:

$$\mathbf{D}(\mathbf{k}) \sim \mathbf{G}^{-1}(\mathbf{k}) \tag{43}$$

The missing coefficient is expressed in terms of the averaged generalized velocity square. Let us consider

$$\widetilde{\Upsilon}_{mn} = \sqrt{\langle \widetilde{\upsilon}_m \widetilde{\upsilon}_n\rangle} = \sqrt{\left\langle \sum_i \widetilde{\upsilon}_{i,m}\widetilde{\upsilon}_{i,n}\right\rangle}, \tag{44}$$

where $\widetilde{\upsilon}_{i,m}$ and $\widetilde{\upsilon}_{i,n}$ are the components of generalized velocities vector. Their number is equal to the number of the CG lattice degrees of freedom. Summation in (44) is carried over the grains i. Let us then introduce the respective tensor $\widetilde{\boldsymbol{\Upsilon}}$. Due to the independence of the generalized coordinates, its non-diagonal components vanish, so formula (44) yields to

$$\widetilde{\Upsilon}_{mn} = \langle \widetilde{\upsilon}_m \widetilde{\upsilon}_n\rangle \delta_{mn}, \tag{45}$$

where δ_{mn} is Kronecker delta.

Hence, the Eq. (43) takes the form

$$\mathbf{D}(\mathbf{k}) = \widetilde{\boldsymbol{\Upsilon}} \cdot \left[\mathbf{G}^{-1}(\mathbf{k})\right] \cdot \widetilde{\boldsymbol{\Upsilon}} \tag{46}$$

The phonon spectrum is obtained by solving the eigenvalues problem for $\mathbf{D}(\mathbf{k})$ for different $\mathbf{k}$. In the simulation the Green's tensor is averaged over $1060T_0$ to smooth the results.

Figure 4 shows the phonon dispersion curves for chains with (a) two and (b) three atoms in a grain subject to 3D motion. Phonon spectrum for grains (black dots) is compared with that for a monoatomic chain (red lines). The equations of motion

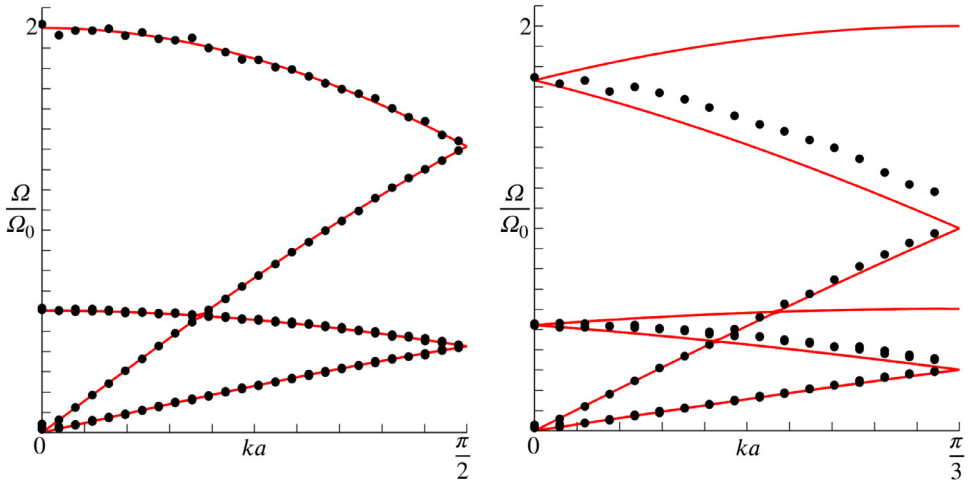

(a) Two atoms per grain, $L = 2a$. (b) Three atoms per grain, $L = 3a$.

Fig. 4. Phonon spectrum for the monoatomic chain (3D motion): analytical solution (red lines) and simulation results for CG chain (black dots). (For interpretation of the references to colour in this figure legend, the reader is referred to the web version of this article.)

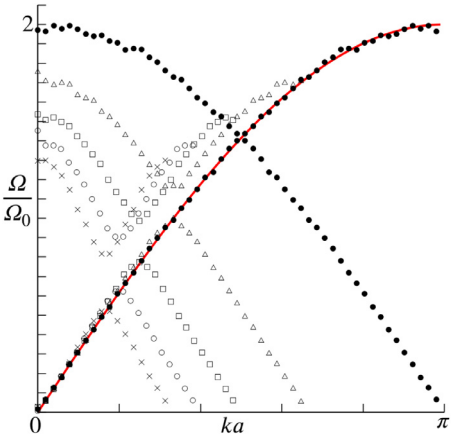

Fig. 5. Phonon spectrum for the monoatomic chain (1D motion): analytical solution (red line) and simulation results for CG chain with 2 atoms per grain (black dots), 3 atoms per grain (black triangles), 4 atoms per grain (black squares), 5 atoms per grain (black circles), and 6 atoms per grain (black crosses). (For interpretation of the references to colour in this figure legend, the reader is referred to the web version of this article.)

for the CG chain with two atoms per grain are given in Section 3. As far as the analytical solution is concerned, the phonon spectrum is determined on the basis of the respective number of atoms, i.e. two or three. Hence, the lattice constants of the original chains L match those of CG chains. This leads to the appearance of auxiliary curves shifted relative to each other by 2π, because we solve the system of the two/three identical equations for two/three neighboring particles. Due to the symmetry, dispersion curves that correspond to the motion along $\mathbf{e}_y$ and $\mathbf{e}_z$ coincide. In order to ensure the stability of the system, the chain is pre-stretched by 10%.

The results of CG modeling for pure one-dimensional case for different grain size are shown in Fig. 5. It demonstrates that the diatomic elastic grains representing three and more atoms, allow obtaining only part of the original spectrum. So, the larger grains are used, the longer waves should be considered to obtain the correct results.

As already noted in the introduction, the stiffness of the bonds between the grains in the deformable model does not change, whereas in the rigid grains it has to be reduced to comply with the overall stiffness of the original lattice. Thus, the rigid grains approach leads to the incorrect prediction of the phonon spectra of the original lattice, whereas the solid grains ensure a better match (see Fig. 6).

Complex CG chain To conclude this paper, let us apply the proposed simulation method to complex lattices. Consider an originally diatomic chain consisting of alternating atoms and bonds between them shown in Fig. 7a. There are two ways to combine the atoms into the grains: we can either take even or odd number of atoms. In the first case the resulting CG chain will be “monoatomic” (see Fig. 7b), whereas in the second case it will also be “diatomic” as the original one (see Fig. 7c). In what follows we consider a diatomic chain where we double the masses of even atoms and halve the even springs’

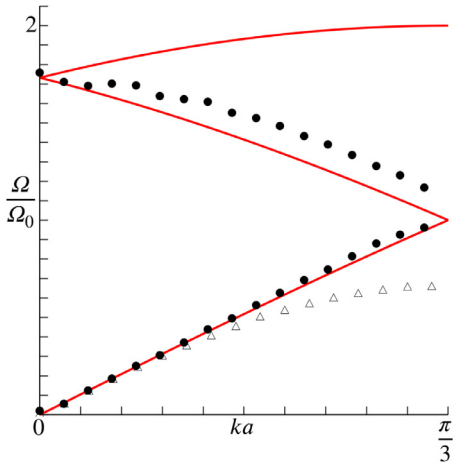

Fig. 6. Phonon spectrum for the monoatomic chain (1D motion): analytical solution (red line), solid grains consisting of three atoms (black dots), ridid grains consisting of three atoms (black triangles). (For interpretation of the references to colour in this figure legend, the reader is referred to the web version of this article.)

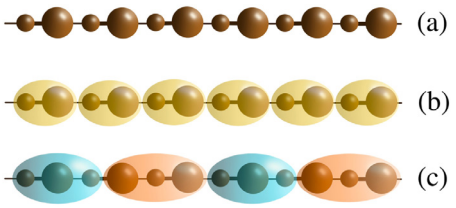

Fig. 7. (a) Original chain consisting of alternating masses, (b) "monoatomic" CG chain (c) "diatomic" CG chain.

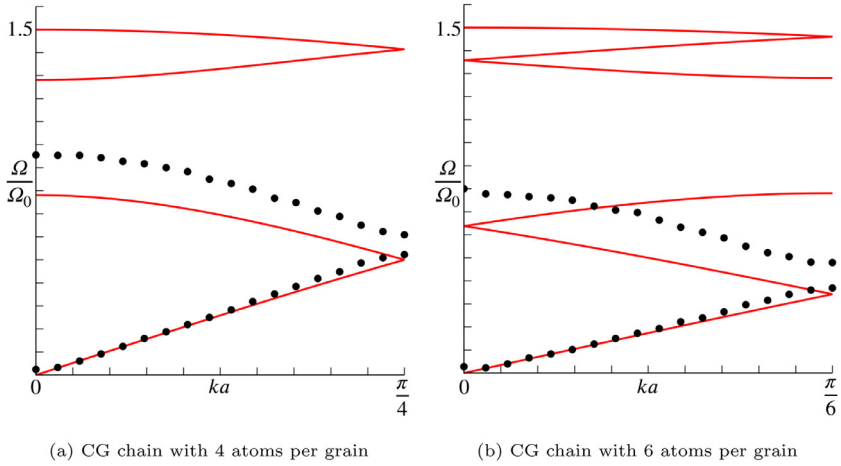

Fig. 8. Phonon spectrum for the diatomic chain (1D motion): analytical solution (red lines) and simulation results for "monoatomic" CG chains. (For interpretation of the references to colour in this figure legend, the reader is referred to the web version of this article.)

stiffnesses compared to the monoatomic chain, i.e. for the odd bonds and atoms $c_i = c_0$, $m_i = m_0$, and for the even bonds and atoms $c_i = 0.5c_0$, $m_i = 2m_0$.

Following a similar procedure, we obtain the phonon spectra for both types of grains. Figure 8 shows the results for the "monoatomic" CG chain. As in case of an originally monoatomic chain, a CG chain with two atoms per grain provides the best fit (not shown in the figures), whereas the more atoms are combined in the grains, the longer waves allow to obtain satisfactory results. The "diatomic" CG chain has the similar features (see Fig. 9) as far as the acoustic branches are concerned, however, the optic branches lie closer to the analytical solution, than those of the "monoatomic" CG chain. Dispersion curves are compared with the analytical solution for a diatomic chain determined on basis of the respective

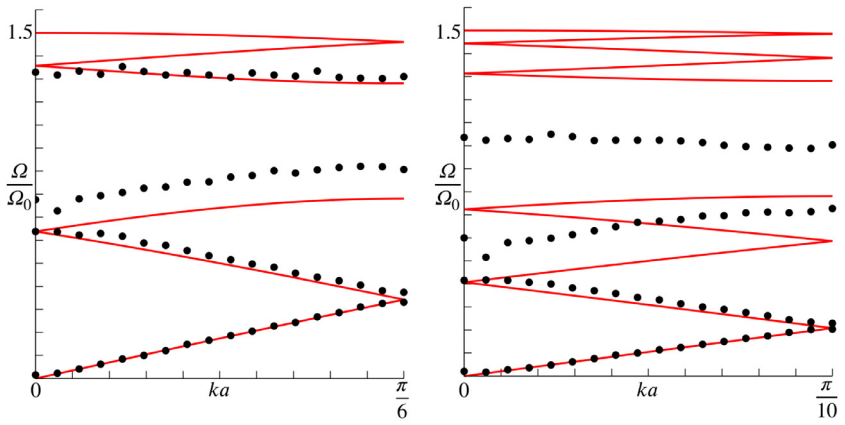

(a) CG chain with 3 atoms per grain (b) CG chain with 5 atoms per grain

Fig. 9. Phonon spectrum for the diatomic chain (1D motion): analytical solution (red lines) and simulation results for "diatomic" CG chains. (For interpretation of the references to colour in this figure legend, the reader is referred to the web version of this article.)

number of atoms, so that the lattice parameters are equal. This leads to the appearance of auxiliary curves shifted relative to each other by 2π. Note, that for "diatomic" CG chain the lattice parameter doubles compared to "monoatomic" CG chain.

6. Concluding remarks

We have developed the general principles of a novel coarse–grained method referred to as HiDRA, formulated upon the representation of atomic structure as a set of rigid and solid grains. The general equations of motion and interaction between the grains were obtained in closed form. Next, we used these equations for numerical simulations with a particle dynamics method close to the discrete (or distinct) element method with non-spherical particles. Still, unlike the methods above, which base on the solution of two vector equations of motion, we have three equations with a uniform strain of the grain as an independent variable. Quaternions formalism was employed to take the rotational degrees of freedom into account.

As a first step, the method was applied to study the atomic chain dynamics in 1D and 3D space. General equations of motion were reduced to describe a chain consisting of coarse grains. It was shown that the effective elastic properties obtained using the CG model fully comply with those of the atomistic model. However, the dynamical properties investigated with the phonon spectra can vary significantly. In the case of the coarse grains, these spectra were obtained with the original procedure. The dynamics of monoatomic and diatomic chains were investigated with grains containing from 2 to 6 atoms. For 3-atomic grains, the HiDRA model is perfectly bounded by two effective analytic models. Dispersion curves show that the larger the grain size is, the longer are the waves that can be described accurately.

The chain of one-dimensional grains considered in this paper has various practical applications. It can be used to simulate biomolecular chains, polymers, textile fibers, etc. However, the general equations of the presented method can be successfully applied for simulations of 2D and 3D objects such as crystal lattices and fiber networks, which is a topic for future research.

Declaration of Competing Interest

The authors declare that they have no known competing financial interests or personal relationships that could have appeared to influence the work reported in this paper.

Acknowledgements

The authors are grateful to M.Sc. Daria Orlova for her kind help with the paper's artwork. The authors would also like to express their appreciation to Prof. Anton Krivtsov for inspiration and insightful suggestions. Dr. Ekaterina Podolskaya appreciates the partial support of the work by the Ministry of Science and Higher Education of the Russian Federation as part of the World-class Research Center program: Advanced Digital Technologies (contract No. 075-15-2020-934 dated 17.11.2020).

Appendix A

Euler-Lagrange equations of motion used in the present derivation take the form:

$$\frac{\mathrm{d}}{\mathrm{d}t}\left(\frac{\partial T_i}{\partial \dot{q}_i}\right) - \frac{\partial T_i}{\partial q_i} = -\frac{\partial U_i}{\partial q_i},$$

where q_i and $\dot{q}_i$ denote the generalized coordinates and the respective rates.

Let us calculate the required derivatives of the kinetic energy (3) and potential energy (4).

From formula (2) it follows that the kinetic energy of grain i depends on the center of mass velocity $\dot{\mathbf{r}}_i$, its angular velocity $\boldsymbol{\omega}_i$, strain $\boldsymbol{\varepsilon}_i$, and strain rate $\dot{\varepsilon}_i$, whereas the dependence on $\mathbf{P}_i$ vanishes after the respective multiplication. The potential energy depends only on the all three generalized coordinates.

First, let us write down the derivative of T_i with respect to $\dot{\mathbf{r}}_i$:

$$\begin{aligned}\frac{\partial T_i}{\partial \dot{\mathbf{r}}_i} &= \sum_\alpha m_\alpha \dot{\mathbf{r}}_\alpha \cdot \frac{\partial \dot{\mathbf{r}}_\alpha}{\partial \dot{\mathbf{r}}_i} = \sum_\alpha m_\alpha \left(\dot{\mathbf{r}}_i + \mathbf{P}_i \cdot (\boldsymbol{\omega}_i \times \mathbf{r}_{i\alpha}) + \mathbf{P}_i \mathbf{r}^0_{i\alpha} \cdot\cdot \dot{\boldsymbol{\varepsilon}}_i\right) \\ &= \sum_\alpha m_\alpha \dot{\mathbf{r}}_i + \mathbf{P}_i \cdot \left(\boldsymbol{\omega}_i \times \sum_\alpha m_\alpha \mathbf{r}_{i\alpha}\right) + \mathbf{P}_i \sum_\alpha m_\alpha \mathbf{r}^0_{i\alpha} \cdot\cdot \dot{\boldsymbol{\varepsilon}}_i = \dot{\mathbf{r}}_i \sum_\alpha m_\alpha\end{aligned} \tag{47}$$

This trivial result, combined with the derivative of U_i with respect to $\mathbf{r}_i$, bearing (5) in mind,

$$\frac{\partial U_i}{\partial \mathbf{r}_i} = -\sum_{j\neq i} \mathbf{F}_{ij} \tag{48}$$

leads to the **first equation** (8)

$$\ddot{\mathbf{r}}_i \sum_\alpha m_\alpha = \sum_{j\neq i} \mathbf{F}_{ij} \tag{49}$$

Then, the derivative of T_i with respect to $\boldsymbol{\omega}_i$ is:

$$\begin{aligned}\frac{\partial T_i}{\partial \boldsymbol{\omega}_i} &= \sum_\alpha m_\alpha \dot{\mathbf{r}}_\alpha \cdot \frac{\partial \dot{\mathbf{r}}_\alpha}{\partial \boldsymbol{\omega}_i} = -\sum_\alpha m_\alpha \dot{\mathbf{r}}_\alpha \cdot \mathbf{P}_i \cdot (\mathbf{r}_{i\alpha} \times \mathbf{E}) \\ &= \sum_\alpha m_\alpha \left(r^2_{i\alpha}\mathbf{E} - \mathbf{r}_{i\alpha}\mathbf{r}_{i\alpha}\right) \cdot \boldsymbol{\omega}_i - \dot{\boldsymbol{\varepsilon}}_i \cdot\cdot \left(\sum_\alpha m_\alpha \mathbf{r}_{i\alpha}\mathbf{r}^0_{i\alpha} \times \mathbf{E}\right).\end{aligned} \tag{50}$$

Introducing the inertia tensors (11), we can calculate the next derivative

$$\begin{aligned}\frac{\mathrm{d}}{\mathrm{d}t}\left(\frac{\partial T_i}{\partial \boldsymbol{\omega}_i}\right) &= \sum_\alpha m_\alpha \left[2\left(\mathbf{r}_{i\alpha} \cdot \dot{\boldsymbol{\varepsilon}}_i \cdot \mathbf{r}^0_{i\alpha}\right)\mathbf{E} - \left(\dot{\boldsymbol{\varepsilon}}_i \cdot \mathbf{r}^0_{i\alpha}\right)\mathbf{r}_{i\alpha} - \mathbf{r}_{i\alpha}\left(\dot{\boldsymbol{\varepsilon}}_i \cdot \mathbf{r}^0_{i\alpha}\right)\right] \cdot \boldsymbol{\omega}_i \\ &\quad + \sum_\alpha m_\alpha \left(r^2_{i\alpha}\mathbf{E} - \mathbf{r}_{i\alpha}\mathbf{r}_{i\alpha}\right) \cdot \dot{\boldsymbol{\omega}}_i - \dot{\boldsymbol{\varepsilon}}_i \cdot\cdot \left(\sum_\alpha m_\alpha \dot{\boldsymbol{\varepsilon}}_i \cdot \mathbf{r}^0_{i\alpha}\mathbf{r}^0_{i\alpha} \times \mathbf{E}\right) \\ &\quad - \ddot{\boldsymbol{\varepsilon}}_i \cdot\cdot \left(\widehat{\mathbf{J}}^T_i \times \mathbf{E}\right) = \mathbf{J}_i \cdot \dot{\boldsymbol{\omega}}_i + \left(2\dot{\boldsymbol{\varepsilon}}_i \cdot \widehat{\mathbf{J}}_i\mathbf{E} - \dot{\boldsymbol{\varepsilon}}_i \cdot \widehat{\mathbf{J}}_i - \widehat{\mathbf{J}}_i \cdot \dot{\boldsymbol{\varepsilon}}_i\right) \cdot \boldsymbol{\omega}_i + \dot{\boldsymbol{\varepsilon}}_i \cdot\cdot \left(\dot{\boldsymbol{\varepsilon}}_i \cdot \widetilde{\mathbf{J}}_i \times \mathbf{E}\right) - \ddot{\boldsymbol{\varepsilon}}_i \cdot\cdot \left(\widehat{\mathbf{J}}^T_i \times \mathbf{E}\right)\end{aligned} \tag{51}$$

As far as the potential energy is concerned, the respective derivative takes the form

$$\frac{\partial U_i}{\partial \boldsymbol{\phi}_i} = -\sum_{j\neq i} \mathbf{M}_{ij}, \tag{52}$$

so the **second equation** of motion (9) is

$$\mathbf{J}_i \cdot \dot{\boldsymbol{\omega}}_i + \left(2\dot{\boldsymbol{\varepsilon}}_i \cdot \widehat{\mathbf{J}}_i\mathbf{E} - \dot{\boldsymbol{\varepsilon}}_i \cdot \widehat{\mathbf{J}}_i - \widehat{\mathbf{J}}_i \cdot \dot{\boldsymbol{\varepsilon}}_i\right) \cdot \boldsymbol{\omega}_i + + \dot{\boldsymbol{\varepsilon}}_i \cdot\cdot \left(\dot{\boldsymbol{\varepsilon}}_i \cdot \widetilde{\mathbf{J}}_i \times \mathbf{E}\right) - \ddot{\boldsymbol{\varepsilon}}_i \cdot\cdot \left(\widehat{\mathbf{J}}^T_i \times \mathbf{E}\right) = \sum_{j\neq i} \mathbf{M}_{ij} \tag{53}$$

Let us note that for small rotations considered in this work $\dot{\boldsymbol{\phi}}_i \equiv \boldsymbol{\omega}_i$.

Finally, let us turn to the derivatives with respect to strain tensor $\boldsymbol{\varepsilon}_i$

$$\begin{aligned}\frac{\partial T_i}{\partial \boldsymbol{\varepsilon}_i} &= \frac{1}{2}\sum_\alpha m_\alpha \frac{\partial}{\partial \boldsymbol{\varepsilon}_i}(\dot{\mathbf{r}}_\alpha \cdot \dot{\mathbf{r}}_\alpha) \\ &= \frac{1}{2}\sum_\alpha m_\alpha \dot{\mathbf{r}}_\alpha \cdot \left[\mathbf{P}_i \cdot (\boldsymbol{\omega}_i \times \mathbf{e}_r)\mathbf{r}^0_{i\alpha}\mathbf{e}_r + \mathbf{P}_i \cdot (\boldsymbol{\omega}_i \times \mathbf{e}_r)\mathbf{e}_r\mathbf{r}^0_{i\alpha}\right] \\ &= \frac{1}{2}\sum_\alpha m_\alpha \left[\omega_i^2\left(\mathbf{r}^0_{i\alpha}\mathbf{r}_{i\alpha} + \mathbf{r}_{i\alpha}\mathbf{r}^0_{i\alpha}\right) - \boldsymbol{\omega}_i \cdot \mathbf{r}_{i\alpha}\mathbf{r}^0_{i\alpha}\boldsymbol{\omega}_i - \boldsymbol{\omega}_i\mathbf{r}^0_{i\alpha}\mathbf{r}_{i\alpha} \cdot \boldsymbol{\omega}_i\right] + \frac{1}{2}\sum_\alpha m_\alpha \dot{\boldsymbol{\varepsilon}}_i \cdot\cdot (\boldsymbol{\omega}_i \times \mathbf{e}_r)\mathbf{r}^0_{i\alpha}\left[\mathbf{r}^0_{i\alpha}\mathbf{e}_r + \mathbf{e}_r\mathbf{r}^0_{i\alpha}\right] \\ &= \frac{1}{2}\left[\omega_i^2\left(\widehat{\mathbf{J}}_i + \widehat{\mathbf{J}}^T_i\right) - \boldsymbol{\omega}_i \cdot \widehat{\mathbf{J}}^T_i\boldsymbol{\omega}_i - \boldsymbol{\omega}_i\widehat{\mathbf{J}}_i \cdot \boldsymbol{\omega}_i\right] + \frac{1}{2}\sum_\alpha m_\alpha \dot{\boldsymbol{\varepsilon}}_i \cdot\cdot (\boldsymbol{\omega}_i \times \mathbf{e}_r)\mathbf{r}^0_{i\alpha}\left[\mathbf{r}^0_{i\alpha}\mathbf{e}_r + \mathbf{e}_r\mathbf{r}^0_{i\alpha}\right]\end{aligned} \tag{54}$$

and strain rate tensor $\dot{\varepsilon}_i$

$$\begin{aligned}\frac{\partial T_i}{\partial \dot{\boldsymbol{\varepsilon}}_i} &= \frac{1}{2}\sum_\alpha m_\alpha \frac{\partial}{\partial \dot{\boldsymbol{\varepsilon}}_i}(\dot{\mathbf{r}}_\alpha \cdot \dot{\mathbf{r}}_\alpha) = \frac{1}{2}\sum_\alpha m_\alpha \dot{\mathbf{r}}_\alpha \cdot \left(P_{i,r,s}\mathbf{e}_r \mathbf{r}^0_{i\alpha}\mathbf{e}_s + \mathbf{P}_i \mathbf{r}^0_{i\alpha}\right)\\ &= \frac{1}{2}\sum_\alpha m_\alpha \left[\mathbf{r}^0_{i\alpha}(\boldsymbol{\omega}_i \times \mathbf{r}_{i\alpha}) + (\boldsymbol{\omega}_i \times \mathbf{r}_{i\alpha})\mathbf{r}^0_{i\alpha} + \mathbf{r}^0_{i\alpha}\mathbf{r}^0_{i\alpha}\cdot\dot{\boldsymbol{\varepsilon}}_i + \dot{\boldsymbol{\varepsilon}}_i \cdot \mathbf{r}^0_{i\alpha}\mathbf{r}^0_{i\alpha}\right]\\ &= \frac{1}{2}\sum_\alpha m_\alpha \left[\boldsymbol{\omega}_i \times \mathbf{r}_{i\alpha}\mathbf{r}^0_{i\alpha} - \mathbf{r}^0_{i\alpha}\mathbf{r}_{i\alpha}\times\boldsymbol{\omega}_i\right] + \frac{1}{2}\sum_\alpha m_\alpha \left[\mathbf{r}^0_{i\alpha}\mathbf{r}^0_{i\alpha}\cdot\dot{\boldsymbol{\varepsilon}}_i + \dot{\boldsymbol{\varepsilon}}_i\cdot\mathbf{r}^0_{i\alpha}\mathbf{r}^0_{i\alpha}\right].\end{aligned} \tag{55}$$

Then,

$$\begin{aligned}\frac{\mathrm{d}}{\mathrm{d}t}\left(\frac{\partial T_i}{\partial \dot{\boldsymbol{\varepsilon}}_i}\right) &= \frac{1}{2}\sum_\alpha m_\alpha \left[\dot{\boldsymbol{\omega}}_i \times \mathbf{r}_{i\alpha}\mathbf{r}^0_{i\alpha} - \mathbf{r}^0_{i\alpha}\mathbf{r}_{i\alpha}\times\dot{\boldsymbol{\omega}}_i\right] + \frac{1}{2}\sum_\alpha m_\alpha \left[\boldsymbol{\omega}_i \times \left(\dot{\boldsymbol{\varepsilon}}_i\cdot\mathbf{r}^0_{i\alpha}\right)\mathbf{r}^0_{i\alpha} - \mathbf{r}^0_{i\alpha}\left(\dot{\boldsymbol{\varepsilon}}_i\cdot\mathbf{r}^0_{i\alpha}\right)\times\boldsymbol{\omega}_i\right]\\ &+ \frac{1}{2}\sum_\alpha m_\alpha \left[\mathbf{r}^0_{i\alpha}\mathbf{r}^0_{i\alpha}\cdot\ddot{\boldsymbol{\varepsilon}}_i + \ddot{\boldsymbol{\varepsilon}}_i\cdot\mathbf{r}^0_{i\alpha}\mathbf{r}^0_{i\alpha}\right] = \frac{1}{2}\left(\dot{\boldsymbol{\omega}}_i\times\widehat{\mathbf{J}}_i^T - \widehat{\mathbf{J}}_i\times\dot{\boldsymbol{\omega}}_i\right)\\ &+ \frac{1}{2}\left(\boldsymbol{\omega}_i\times\dot{\boldsymbol{\varepsilon}}_i\cdot\widetilde{\mathbf{J}}_i - \widetilde{\mathbf{J}}_i\cdot\dot{\boldsymbol{\varepsilon}}_i\times\boldsymbol{\omega}_i\right) + \frac{1}{2}\left(\ddot{\boldsymbol{\varepsilon}}_i\cdot\widetilde{\mathbf{J}}_i + \widetilde{\mathbf{J}}_i\cdot\ddot{\boldsymbol{\varepsilon}}_i\right)\end{aligned} \tag{56}$$

Passing over to the derivative of the potential energy with respect to $\boldsymbol{\varepsilon}_i$, we get

$$\frac{\partial U_i}{\partial \boldsymbol{\varepsilon}_i} = \sum_\alpha \frac{\partial U_i}{\partial \mathbf{r}_\alpha}\cdot\frac{\partial \mathbf{r}_\alpha}{\partial \boldsymbol{\varepsilon}_i} + V\boldsymbol{\sigma}_i^{int}, \qquad \boldsymbol{\sigma}_i^{int} = {}^4\mathbf{C}\cdot\cdot\boldsymbol{\varepsilon}_i \tag{57}$$

Here $\boldsymbol{\sigma}_i^{int}$ stands for the *internal* stress tensor which describes the stress state inside the grain.

Further simplification, bearing (5) and (6) in mind, leads to

$$\begin{aligned}\frac{\partial U_i}{\partial \mathbf{r}_\alpha}\cdot\frac{\partial \mathbf{r}_\alpha}{\partial \boldsymbol{\varepsilon}_i} &= -\sum_{j\neq i,\beta}\mathbf{F}_{\alpha\beta}\cdot\frac{\partial \mathbf{r}_\alpha}{\partial \boldsymbol{\varepsilon}_i} = -\frac{1}{2}\sum_{j\neq i,\beta}\mathbf{F}_{i,\alpha\beta}\cdot\mathbf{P}_i^T\cdot P_{i,r,s}\mathbf{e}_r\mathbf{r}^0_{i\alpha}\mathbf{e}_s -\\ &- \frac{1}{2}\sum_{j\neq i,\beta}\mathbf{F}_{i,\alpha\beta}\cdot\mathbf{P}_i^T\cdot\mathbf{P}_i\mathbf{r}^0_{i\alpha} = -\frac{1}{2}\sum_{j\neq i,\beta}\left[\mathbf{r}^0_{i\alpha}\mathbf{F}_{i,\alpha\beta} + \mathbf{F}_{i,\alpha\beta}\mathbf{r}^0_{i\alpha}\right] \equiv -V\boldsymbol{\sigma}_i^{ext},\end{aligned} \tag{58}$$

where the *external* stress tensor $\boldsymbol{\sigma}_i^{ext}$ is introduced, and $\mathbf{F}_{i,\alpha\beta}$ is calculated in the frame associated with the grain, so we obtain the **third equation** of motion (10):

$$\begin{aligned}&\frac{1}{2}\left(\ddot{\boldsymbol{\varepsilon}}\right]_i\cdot\widetilde{\mathbf{J}}_i + \widetilde{\mathbf{J}}_i\cdot\ddot{\boldsymbol{\varepsilon}}_i\right) + \frac{1}{2}\left(\dot{\boldsymbol{\omega}}_i\times\widehat{\mathbf{J}}_i^T - \widehat{\mathbf{J}}_i\times\dot{\boldsymbol{\omega}}_i\right) + \frac{1}{2}\left(\boldsymbol{\omega}_i\times\dot{\boldsymbol{\varepsilon}}_i\cdot\widetilde{\mathbf{J}}_i - \widetilde{\mathbf{J}}_i\cdot\dot{\boldsymbol{\varepsilon}}_i\times\boldsymbol{\omega}_i\right)\\ &-\frac{1}{2}\left[\omega_i^2\left(\widehat{\mathbf{J}}_i + \widehat{\mathbf{J}}_i^T\right) - \boldsymbol{\omega}_i\cdot\widehat{\mathbf{J}}_i^T\boldsymbol{\omega}_i - \boldsymbol{\omega}_i\widehat{\mathbf{J}}_i\cdot\boldsymbol{\omega}_i\right] - \frac{1}{2}\sum_\alpha m_\alpha\dot{\boldsymbol{\varepsilon}}_i\cdot\cdot(\boldsymbol{\omega}_i\times\mathbf{e}_r)\mathbf{r}^0_{i\alpha}\left[\mathbf{r}^0_{i\alpha}\mathbf{e}_r + \mathbf{e}_r\mathbf{r}^0_{i\alpha}\right] = V\left(\boldsymbol{\sigma}_i^{int} - \boldsymbol{\sigma}_i^{ext}\right)\end{aligned} \tag{59}$$

References

Abraham, F. F., Broughton, J. Q., Bernstein, N., & Kaxiras, E. (1998). Spanning the continuum to quantum length scales in a dynamic simulation of brittle fracture. *EPL (Europhysics Letters), 44*(6), 783.

Allen, M., & Tildesley, D. (1989). *Computer simulation of liquids*. Oxford University Press.

Altmann, S. (1986). *Rotations, quaternions, and double groups*. Clarendon Press, Oxford.

Care, C., & Cleaver, D. (2005). Computer simulation of liquid crystals. *Reports on Progress in Physics, 68*(11), 2665.

Chen, Y., & Lee, J. (2005). Atomistic formulation of a multiscale field theory for nano/micro solids. *Philosophical Magazine, 85*(33–35), 4095–4126.

Chen, Y., Lee, J. D., & Eskandarian, A. (2004). Atomistic viewpoint of the applicability of microcontinuum theories. *International Journal of Solids and Structures, 41*(8), 2085–2097.

Chen, Y., Zimmerman, J., Krivtsov, A., & McDowell, D. L. (2011). Assessment of atomistic coarse-graining methods. *International Journal of Engineering Science, 49*(12), 1337–1349.

Cundall, P., & Strack, O. (1979). A discrete numerical model for granular assemblies. *Geotechnique, 29*(1), 47–65.

Eringen, A. C., & Suhubi, E. (1964). Nonlinear theory of simple micro-elastic solidsi. *International Journal of Engineering Science, 2*(2), 189–203.

Gautieri, A., Russo, A., Vesentini, S., Redaelli, A., & Buehler, M. J. (2010). Coarse-grained model of collagen molecules using an extended MARTINI force field. *Journal of Chemical Theory and Computation, 6*(4), 1210–1218.

Gerberich, W., Tadmor, E. B., Kysar, J., Zimmerman, J. A., Minor, A. M., Szlufarska, I., … Ballarini, R. (2017). Case studies in future trends of computational and experimental nanomechanics. *Journal of Vacuum Science & Technology A: Vacuum, Surfaces, and Films, 35*(6), 060801.

Ivanova, E., Krivtsov, A., & Morozov, N. (2007). Derivation of macroscopic relations of the elasticity of complex crystal lattices taking into account the moment interactions at the microlevel. *Journal of Applied Mathematics and Mechanics, 71*(4), 543–561.

Ivanova, E. (2018). On the Use of the Continuum Mechanics Method for Describing Interactions in Discrete Systems with Rotational Degrees of Freedom. *Journal of Elasticity, 133*, 155–199. https://doi.org/10.1007/s10659-018-9676-3.

Kmiecik, S., Gront, D., Kolinski, M., Wieteska, L., Dawid, A. E., & Kolinski, A. (2016). Coarse-grained protein models and their applications. *Chemical Reviews, 116*(14), 7898–7936.

Kochmann, D. M., & Amelang, J. S. (2016). The quasicontinuum method: Theory and applications. In *Multiscale materials modeling for nanomechanics* (pp. 159–193). Springer.

Kong, L. T. (2011). Phonon dispersion measured directly from molecular dynamics simulations. *Computer Physics Communications, 182*(10), 2201–2207.

Levitt, M., & Chothia, C. (1976). Structural patterns in globular proteins. *Nature, 261*(5561), 552–558.

Liu, W. K., Park, H. S., Qian, D., Karpov, E. G., Kadowaki, H., & Wagner, G. J. (2006). Bridging scale methods for nanomechanics and materials. *Computer Methods in Applied Mechanics and Engineering, 195*(13–16), 1407–1421.

Miller, R. E., & Tadmor, E. B. (2002). The quasicontinuum method: Overview, applications and current directions. *Journal of Computer-Aided Materials Design, 9*(3), 203–239.
Noid, W. G. (2013). Perspective: Coarse-grained models for biomolecular systems. *The Journal of Chemical Physics, 139*(9), 09B201_1.
Ostanin, I., Dumitrică, T., Eibl, S., & Rüde, U. (2019). Size-independent mechanical response of ultrathin carbon nanotube films in mesoscopic distinct element method simulations. *Journal of Applied Mechanics, 86*(12).
Panchenko, A. Y., Podolskaya, E., & Berinskii, I. (2020). Coarse–grained model based on rigid grains interaction for single layer molybdenum disulfide. *Mechanics Research Communications, 105*, 103515.
Psakhie, S. G., Shilko, E., Grigoriev, A., Astafurov, S., Dimaki, A., & Smolin, A. Y. (2014). A mathematical model of particle–particle interaction for discrete element based modeling of deformation and fracture of heterogeneous elastic–plastic materials. *Engineering Fracture Mechanics, 130*, 96–115.
Psakhie, S. G., Shilko, E., Smolin, A. Y., Dimaki, A., Dmitriev, A., Konovalenko, I. S., … Zavshek, S. (2011). Approach to simulation of deformation and fracture of hierarchically organized heterogeneous media, including contrast media. *Physical Mesomechanics, 14*(5–6), 224–248.
Rapaport, D. C. (2004). *The art of molecular dynamics simulation*. Cambridge University Press.
Rojek, J., Zubelewicz, A., Madan, N., & Nosewicz, S. (2018). The discrete element method with deformable particles. *International Journal for Numerical Methods in Engineering, 114*(8), 828–860.
Rudd, R. E., & Broughton, J. Q. (1998). Coarse-grained molecular dynamics and the atomic limit of finite elements. *Physical Review B, 58*(10), R5893.
Shi, X., Kong, Y., & Gao, H. (2008). Coarse grained molecular dynamics and theoretical studies of carbon nanotubes entering cell membrane. *Acta Mechanica Sinica, 24*(2), 161–169.
Shilkrot, L., Miller, R. E., & Curtin, W. A. (2004). Multiscale plasticity modeling: Coupled atomistics and discrete dislocation mechanics. *Journal of the Mechanics and Physics of Solids, 52*(4), 755–787.
Wang, X., & Lee, J. D. (2010). Micromorphic theory: A gateway to nano world. *International Journal of Smart and Nano Materials, 1*(2), 115–135.
Warshel, A., & Levitt, M. (1976). Theoretical studies of enzymic reactions: Dielectric, electrostatic and steric stabilization of the carbonium ion in the reaction of lysozyme. *Journal of Molecular Biology, 103*(2), 227–249.
Wilson, M. R. (2005). Progress in computer simulations of liquid crystals. *International Reviews in Physical Chemistry, 24*(3–4), 421–455.
Xiao, S., & Belytschko, T. (2004). A bridging domain method for coupling continua with molecular dynamics. *Computer Methods in Applied Mechanics and Engineering, 193*(17–20), 1645–1669.